HHS Public Access

Author manuscript

J Mol Cell Cardiol. Author manuscript; available in PMC 2019 September 01.

Published in final edited form as:

J Mol Cell Cardiol. 2018 September ; 122: 88–97. doi:10.1016/j.yjmcc.2018.08.009.

Cardiac-Specific Knockout of Lmod2 Results in a Severe Reduction in Myofilament Force Production and Rapid Cardiac Failure

Christopher T. Pappas[#a], **Gerrie P. Farman**[#a], **Rachel M. Mayfield**[a], **John P. Konhilas**[b], and **Carol C. Gregorio**[a]

[a]Department of Cellular and Molecular Medicine, and Sarver Molecular Cardiovascular Research Program, University of Arizona, Tucson, AZ

[b]Department of Physiology, and Sarver Molecular Cardiovascular Research Program, University of Arizona, Tucson, AZ

[#] These authors contributed equally to this work.

Abstract

Leiomodin-2 (Lmod2) is a striated muscle-specific actin binding protein that is implicated in assembly of thin filaments. The necessity of Lmod2 in the adult mouse and role it plays in the mechanics of contraction are unknown. To answer these questions, we generated cardiac-specific conditional Lmod2 knockout mice (cKO). These mice die within a week of induction of the knockout with severe left ventricular systolic dysfunction and little change in cardiac morphology. Cardiac trabeculae isolated from cKO mice have a significant decrease in maximum force production and a blunting of myofilament length-dependent activation. Thin filaments are non-uniform and substantially reduced in length in cKO hearts, affecting the functional overlap of the thick and thin filaments. Remarkably, we also found that Lmod2 levels are directly linked to thin filament length and cardiac function *in vivo,* with a low amount (<20%) of Lmod2 necessary to maintain cardiac function. Thus, Lmod2 plays an essential role in maintaining proper cardiac thin filament length in adult mice, which in turn is necessary for proper generation of contractile force. Dysregulation of thin filament length in the absence of Lmod2 contributes to heart failure.

Keywords

actin-thin filaments; cardiomyopathy; sarcomere

Address correspondence to: Christopher T. Pappas, PhD, Dept. of Cellular and Molecular Medicine, 1656 E. Mabel St., MRB 323, Tucson, Arizona 85724, USA. Tel: 520-626-5209, Fax: 520-626-7600, ctpappas@email.arizona.edu.

Disclosures

None

1. Introduction

At the core of muscle contraction is the orderly arrangement of myosin-containing thick and actin-containing thin filaments. To maintain proper force production the lengths of the filaments need to be strictly regulated. Congruent with this requirement, mutations within either the proteins of the thin filament, or those that regulate thin filament length greatly impact muscle force production and can lead to disease [1, 2].

Thin filament length is determined by a combination of proteins that control actin polymerization and stability of the filament, though the entirety of proteins involved and how they function together is not fully understood. Central among them are the tropomodulins (Tmods), with Tmod1 representing the predominate isoform in the heart [3]. Tmods use two actin- and two tropomyosin-binding sites to effectively cap and limit actin dynamics at the pointed end of the thin filament [4–7].

Proteins that are closely related to the Tmods, named the leiomodins (Lmods), have also been implicated in regulating actin filaments in muscle. The major cardiac isoform is Lmod2 [3]. Likely owing to: 1) the lack of a second TM-binding site, 2) a modified second actin-biding site and/or 3) the addition of a C-terminal extension with a third actin binding site within Lmod2, Lmod2 and Tmod1 have divergent biochemical functions [8, 9]. Lmod2 is a potent nucleator of actin polymerization *in vitro*, whereas Tmod1 is only able to nucleate at high concentrations [10, 11]. In neonatal cardiomyocytes in culture, overexpression of Lmod2 increases pointed end actin dynamics leading to elongation of the thin filament [12, 13]. Consistent with this function, Lmod2 null mice have abnormally short thin filaments [12]. These mice present with dilated cardiomyopathy and die 2–3 weeks after birth [12].

It is currently unclear how Lmod2's biochemical function reconciles with its observed cellular function. Since the global constitutive knockout mice die before the heart is fully developed it is unknown whether Lmod2 is necessary for cardiac function in the adult. Furthermore, little is known regarding the consequences of the loss of Lmod2 on contractile activity. To address these questions, we generated an inducible heart-specific *Lmod2* knockout mouse (*Lmod2* cKO). *Lmod2* cKO mice die within a week of Lmod2 deletion with severe systolic dysfunction. Our data reveal that these mice have abnormally short, non-uniform thin filaments, resulting in decreased contractile force generation and a reduction in myofilament length-dependent activation, setting into motion a rapid cascade of cellular responses that exacerbates heart dysfunction. We found that a dose-response relationship exists between Lmod2 levels and both thin filament length and cardiac function, with a surprisingly low amount (<20%) of Lmod2 required to maintain cardiac function. Our data also suggest that shorter thin filaments cannot account for the entire contractile force deficit the cKO mice display.

2. Methods

2.1. Generation of *Lmod2* conditional KO mice

All animal procedures were approved by the Institutional Care and Use Committee at the University of Arizona. *Lmod2* cKO mice were generated through gene targeting in 129/S6-

strain embryonic stem cells. Homologous ends for recombination were obtained from the same strain. The gene targeting scheme placed a polyA-deficient pmC1neo gene flanked by flippase recombinase target (FRT) sequences within the first intron. LoxP sites were placed 5' of the 1st exon and 3' of the neo gene (Fig. S1). Targeted ES cells were injected into blastocysts from a C57BL/6J mouse. Floxed Lmod2 mice were then crossed with C57BL/6J mice containing the cardiac-specific alpha myosin heavy chain promoter (Myh6) driving a tamoxifen inducible Cre recombinase (B6.FVB(129)-A1cfTg$^{(Myh6\text{-}cre/Esr1*)1Jmk}$/J, The Jackson Laboratory) [14]. Effective knockout of the Lmod2 gene was achieved by the injection of 30 mg/kg of tamoxifen on three consecutive days.

2.2. Genotyping

Genomic DNA was isolated as previously described [12]. PCR was performed with primers to intron 2 of *Lmod2*. One set of primers (F: 5'- TCCAATGACCACAAATCCAA; R: 5'-CCGGAGATCAGTCTCCTGAA) amplifies a 505-base pair product in the WT allele and a 2050–base pair product in the floxed allele and a second set of primers (F: 5'-CCAGAGTGTGGGTTTGAAGG; R: 5'-CTGGCACTCTGTCGATACCC), amplifies a 405-base pair product only in the floxed allele. PCR conditions were as follows: 95°C for 2 min, [95°C for 30 sec, 61°C for 30 sec, 72°C for 40 sec] repeat 35x, 72°C for 5 min.

2.3. Solutions

The compositions of all solutions were reported previously for trabeculae [15] and single cells [16]. Activating and relaxing solutions were mixed to obtain activating solutions containing between 0.64 and 46.8 μM [Ca^{2+}] (pCa 6.2–4.3).

2.4. Tissue Collection

Mice were administered 100 units of heparin via intraperitoneal injection and, after 5 minutes, anesthetized with isoflurane and sacrificed by cervical dislocation. The heart was then excised, transferred to a dissection dish and perfused retrograde with a modified Krebs-Henseleit solution, containing 118.5 mM NaCl, 5 mM KCl, 2 mM NaH_2PO_4, 1.2 mM $MgSO_4$, 10 mM glucose, and 26.4 mM $NaHCO_3$, as well as an additional 10 mM KCl to inhibit spontaneous contractions. This solution, when aerated at room temperature with a 95% O_2 /5% CO_2 mixture had a pH of 7.4. Only single, isolated, unbranched trabeculae located along the exterior wall of the RV or LV were removed. The muscles were placed into a dish containing skinning solution which is comprised of a standard relaxing solution with 1% (v/v) Triton X-100 [15]. The intraventricular septum (for single cell experiments), atria, RV free wall and LV free wall were also removed and quickly frozen in liquid nitrogen for later use.

2.5. Force/Calcium Relationship

For single fiber mechanics, muscles were incubated in skinning solution for 3–5 hours at 4°C then transferred to fresh relaxing solution. Trabeculae 1–2 mm long, 50300 μm wide, and 50–250 μm thick were attached to aluminum T-clips and mounted on hooks between a silicon strain gauge (model AE801, SenSonor, Horten Norway) and a servomotor (Aurora Scientific model 322; ~0.4ms 99% step response). Prior to activation with calcium,

sarcomere length was set to either 1.95 ± 0.03 μm or 2.25 ± 0.03 μm using the first order diffraction band from a He-Ne laser [17]. If the final maximal calcium activation in the run generated <90% of the force of the initial full activation, the data were discarded. All experiments were performed at 15°C.

Single cell experiments were performed on an inverted microscope stage using an Aurora Scientific 803B permeabilized myocyte apparatus with some slight modifications; a 406A force transducer was used to obtain a wider range of minimum and maximum forces. Permeabilized single cells were acquired by homogenizing ~1/3 of the frozen interventricular septum in skinning solution. The cells were gently pelleted by centrifugation for 3 min at 23 x g. This pellet was then washed, and centrifugation repeated three times with relaxing solution to remove any remaining detergent.

Force-[Ca^{2+}] relationships were fit individually to a modified Hill equation as previously described [15]:

$$F_{rel} = \left[Ca^{2+}\right]^n / \left(EC_{50}{}^n + \left[Ca^{2+}\right]^n\right) \quad (1)$$

where F_{rel} = force as a fraction of maximum force at saturating [Ca^{2+}] (F_{max}), EC_{50} = [Ca^{2+}] where the F_{rel} is half of F_{max}, and n = Hill Coefficient.

2.6. Immunoblots

For total lysate, a portion of LV free wall tissue was homogenized as previously described [12]. For fractionation experiments, LV tissue was minced in cold ringer buffer (150 mM NaCl, 2 mM KCl, 2 mM $MgCl_2$, 10 mM KH_2PO_4, 1 mM EGTA, 0.1% glucose, pH 7.0), then homogenized for ~30 sec at speed 3 with an Ultra-Turrax T8 homogenizer (IKA Works, Inc) in cold rigor buffer (100 mM KCl, 2 mM $MgCl_2$, 10 mM KH_2PO_4, 1 mM EDTA, pH 7.0) plus 1% Triton X-100 and protease inhibitors. Samples were then centrifuged at 3000 x g for 5 min at 4°C and the pellet washed 4x with rigor buffer (1x with Triton X-100 and 3x without). The pellet was then resuspended in lysis buffer (150 mM NaCl, 1.5 mM $MgCl_2$, 1 mM EGTA, 10 mM sodium pyrophosphate, 10 mM sodium fluoride, 0.1 mM sodium deoxycholate, 1% Triton X-100, 1% SDS, 10% (vol/vol) glycerol, 25 mM Hepes, pH 7.4, plus protease inhibitors), and sonicated. Total protein concentrations were normalized, lysate resolved on 8 or 12% SDS gels and transferred to nitrocellulose as previously described [12]. Following transfer, the membrane was blocked with 5% (wt/vol) nonfat dried milk/TBS for 1 h at room temperature and then incubated with primary antibodies in 1% BSA (wt/vol)/TBST overnight at 4° C. Primary antibodies included rabbit polyclonal anti-leiomodin 2 (0.1 μg/mL) (E13; Santa Cruz Biotechnology), rabbit polyclonal anti-CARP1 (Ankrd1) (1:200) (Myomedix) and mouse monoclonal anti-FHL1 (0.5 μg/mL) (ab76912; Abcam). The membranes were then washed 5×5 min in TBST and incubated with fluorescently labelled anti-rabbit IgG (1:40,000) or anti-mouse IgG (1:40,000) (Jackson ImmunoResearch) diluted in 5% milk/TBST for 1 h at room temperature. Blots were imaged and analyzed using a LICOR Odyssey CLx imaging system (LI-COR).

2.7. Phosphoprotein stain

20 μg of LV free wall lysate, prepared as outlined above, was resolved on 4–20% SDS gels and stained for total phosphoprotein with Pro-Q Diamond stain according to the manufacturer's instructions (ThermoFisher). PeppermintStick phosphoprotein molecular weight standard was used to determine protein sizes and as positive/negative controls for correct image adjustment (ThermoFisher). Total protein was determined by staining with Coomassie blue. Gels were imaged using UV transillumination on a G-Box Chemi-XR5 chemiluminescent imaging system (Syngene). Specific gel bands were quantified using ImageJ (NIH).

2.8. Immunofluorescence microscopy

A section of LV free wall was stretched (to effectively resolve thin filament pointed ends), fixed overnight in 4% paraformaldehyde/PBS, extensively washed in PBS, embedded in Tissue-Tek O.C.T. compound (Sakura Finetek) and immediately frozen in 2-methlybutane cooled by liquid N_2. Five μm cryosections were cut and mounted onto gelatin-coated coverslips. Cryosections were permeabilized in 0.2% Triton X-100/PBS for 20 min at room temperature, blocked with 2% BSA plus 1% normal donkey serum/PBS for 1 hour at room temp, and incubated overnight at 4°C with mouse monoclonal anti-α-actinin antibodies (1:200) (EA-53, Sigma). Sections were then washed with PBS for 20 min and incubated with Alexa Fluor 488-conjugated goat antimouse IgG (1:1,000) (ThermoFisher)/PBS for 1.5 h. Texas-Red-conjugated phalloidin (1:50) was used to stain F-actin (ThermoFisher). Sections were washed with PBS for 20 min then mounted onto slides with Aqua Poly/Mount (Polysciences Inc.). Images were captured using a Deltavision RT system (Applied Precision) with a 100× NA 1.3 objective, and a charge-coupled device camera (CoolSNAP HQ; Photometrics). Images were deconvolved using SoftWoRx software and processed using Photoshop CS (Adobe).

2.9. Analysis of Thin Filament Architecture

Thin filament and sarcomere lengths were measured using the DDecon plugin for Image J [18, 19]. The "focus" output of the DDecon plugin was used to determine the uniformity of thin filament distribution (the smaller the value, the more uniform the distribution of thin filament ends). Thin filament arrays that had a focus value within one standard deviation of the mean focus of the control mice (*Lmod2*$^{+/+}$;MCM$^{+/-}$) were included in the mean length measurements.

2.10. Reverse transcription PCR (RT-PCR)

RNA was extracted from LV tissue and cDNA generated as previously described [12]. Expression levels were determined by PCR with GoTaq DNA Polymerase (Promega) on a C100 Touch Thermal Cycler (Biorad). The number of cycles that avoid saturation and allow semi-quantitative comparison of template amounts were determined for each set of primers. Each sample was normalized to ornithine decarboxylase (ODC) and the mean expression of *Lmod2*$^{+/+}$;MCM$^{+/-}$ set to 1. Primers sequences were obtained from qPrimerDepot (NIH) and tested to ensure efficiencies of amplification are nearly equal. Primers included ANF (F: 5-GGGGGTAGGATTGACAGGAT and R: 5-AGGGCTTAGGATCTTTTGCG; 130-base

pair product), BNP (F: 5'-ACAAGATAGACCGGATCGGA and R: 5'ACCCAGGCAGAGTCAGAAAC; 110-base pair product) and SERCA2a (F: 5'AATATGAGCCTGAAATGGGC and R: 5'-TCAGCAGGAACTTTGTCACC; 124-base pair product).

2.11. Echocardiography

Anesthetized mice were placed in dorsal recumbence on a heated (37°C) platform for echocardiography (echo). After attaining a target heart rate of 550 ± 50 bpm, transthoracic echo images were obtained with a Vevo 2100 High Resolution Imaging System (Visual-Sonics) using a model MS-550D transducer array. Images were collected and stored as a digital cine loop for off-line calculations. Standard imaging planes and functional calculations were obtained according to American Society of Echocardiography guidelines. M-mode images at the level of the papillary muscles were used to determine LV wall thicknesses, chamber dimensions and ejection fraction.

2.12. Statistics

All statistical analyses were performed in Prism 7 (Graphpad Software Inc.). Two groups were compared using Student's t-tests (Figs. 3, 6B). Multiple groups were compared using two-way ANOVAs (Figs. 1, 2, 4, 5, S2, S3, S4) with Tukey's post-hoc test. Lines were fit to the data in Figs. 2D, 6C and 7 using linear regression analysis. Correlations in Fig 7. were considered significant if the slopes of the linear regression fits were significantly non-zero. $P < 0.5$ was considered significant. *$P < 0.05$, **$P < 0.01$, ***$P < 0.001$, ****$P < 0.0001$.

3. Results

3.1. Lmod2 cKO mice die with compromised systolic function

In order to study the function of Lmod2 in hearts of adult mice, we generated a mouse with the first exon of *Lmod2* flanked by loxP sequences ($Lmod2^{fl/fl}$) (Fig. S1). These mice were then crossed with MerCreMer mice, which have a tamoxifen inducible cre recombinase whose expression is driven by the cardiac-specific alpha myosin heavy chain promoter ($Lmod2^{fl/fl}$;$MCM^{+/-}$). $Lmod2^{fl/fl}$;$MCM^{+/-}$ mice injected with tamoxifen will be referred to as *Lmod2* cKOs. Tamoxifen administration in the MerCreMer mice results in a well-documented transient cardiomyopathy [20]. Therefore, we made sure to use the minimal tamoxifen dose that results in loss of Lmod2 and included MerCreMer positive mice with wild type alleles of *Lmod2* as a control ($Lmod2^{+/+}$;$MCM^{+/-}$).

Lmod2 cKO mice begin to die within one week of the initial tamoxifen injection. At 5–7 days following the first injection, transthoracic M-mode echocardiography at the level of the papillary muscle revealed a large decrease in systolic performance (Fig. 1A) and very little change in cardiac morphology. There is a slight decrease in diastolic LV wall thickness in the *Lmod2* cKO mice when compared to vehicle treated mice (Fig. 1C, D; note, the change in wall thickness is only significant for the anterior wall). LV enddiastolic internal diameter is not significantly different (p=0.09) (Fig, 1B). However, the eccentricity index, the ratio of chamber diameter to wall thickness in diastole, is marginally increased (Fig, 1E), consistent with cardiac dilation. LV internal diameter is increased and wall thickness decreased in

systole, consistent with a loss of contractility (Fig. S2A-C). Heart rates were not significantly different between groups (Fig. S2D). Thus, loss of Lmod2 in the adult results in rapid cardiac failure with a remarkably small change in cardiac morphology. The change in cardiac morphology appears to be mostly driven by tamoxifen treatment, since it is only significant when the cKO is compared to vehicle-treated (and not tamoxifen-treated) control mice and is subtle enough that it was not noted during dissection, even in mice near death. Immunoblot analysis revealed the cKO mice have no detectable levels of Lmod2, while the *Lmod2*$^{fl/fl}$;MCM$^{+/-}$ mice injected with vehicle alone express only 15 ± 5% of wild-type Lmod2 levels (±SD; n=18; $p<0.0001$, Student's t test) (Fig. 1F). This could be due to disruption of transcriptional regulation by the introduced loxP or neomycin sequences. Interestingly, these mice do not present with any detectable cardiac phenotype (see above).

To learn more about the state of the cKO hearts, we probed for various wellstudied markers of stress associated with cardiomyopathies. Immunoblot analysis revealed that the protein levels of cardiac-specific ankyrin repeat protein (CARP1), which is a stress marker often upregulated in hypertrophic and dilated cardiomyopathies as well as four-and-a-half LIM domains 1 (FHL1), which is also thought to sense biomechanical stress (e.g., [21, 22]), are significantly increased in the hearts of cKO mice compared to control mice (**Fig. S3A**). These results suggest that the hearts of the cKO mice are subjected to significant levels of strain. RT-PCR analysis revealed a significant change in the gene expression of molecular markers of heart failure in both the wild type and *Lmod2*$^{fl/fl}$ mice injected with tamoxifen (**Fig. S3B**). Thus, the control mice show no overt cardiac disease phenotype even though signatures of tamoxifeninduced cardiomyopathy are present.

3.2. Lmod2 cKO mice have remarkably short and broad distribution of thin filament lengths

We next analyzed thin filament structure via deconvolution microcopy. Thin cryosections of stretched-LV free wall were stained with fluorescently-labeled phalloidin, which marks F-actin, and an antibody to α-actinin, which labels the Z-discs (Fig. 2A). The spatial organization of thin filaments were then measured using the Distributed Deconvolution (DDecon) plugin for ImageJ, which provides sub-diffraction limit resolution [18, 19]. *Lmod2* cKO mice have a significantly larger mean focus value, reflecting a decrease in the uniformity of thin filaments within each sarcomere (Fig. 2B). Uniform (example 1) and non-uniform (example 2) thin filament arrays are illustrated in Fig 2A. This result is surprising since it is the first time non-uniform thin filaments have been reported when either Lmod2 or Tmod1 levels are altered. Mean thin filament length is significantly reduced (by ~20%) in the hearts of *Lmod2* cKO mice (Fig. 2C). It has previously been shown that thin filament length varies with sarcomere length, although the underlying cause of this phenomenon is unknown [23]. Therefore, in order to confirm that the observed reduction in thin filament length is not due to a difference in sarcomere length, we plotted thin filament vs. sarcomere lengths (Fig. 2D). Indeed, thin filament length is reduced in cKO hearts (by ~10–12% when calculated using the results of linear regression shown in Fig. 2D).

Supporting the presence of shorter thin filaments, immunoblot analysis of the LV revealed a significant decrease in thin filament components cardiac actin and cardiac troponin I (cTnI)

in the knockout hearts (Fig. 3). Myosin binding protein C (MyBP-C), which is associated with the thick filament, and α-actinin, an integral Z-disc component, were unchanged (Fig. 3), indicating that only thin filaments are altered. A decrease in thin filament components could also result from a reduction in the total number of thin filaments. We reasoned that the amount of cytoskeletal bound Tmod1 would give a good approximation of the number of thin filaments present since Tmod1 interacts with only the pointed end of the thin filament and has a stoichiometry of 1–2 per thin filament [4, 24]. As was observed in total lysate, thin filament proteins were decreased in the insoluble fraction of LV lysate from the cKO mice, while Tmod1 and thick filament/Z-disc components were not significantly changed (Fig. 3). These results indicate that there are shorter, not fewer, thin filaments in the *Lmod2* cKO hearts.

3.3. Lmod2 cKO mice have a reduced calcium activated force response

To examine the impact loss of Lmod2 has on myofibrillar force output and response to calcium we performed single fiber mechanics on chemically skinned fibers. Loss of Lmod2 significantly reduces force at sarcomere lengths of 1.95 and 2.25 μm (**Fig. 4A-D, Table S1**). Furthermore, the change in maximally activated force ΔF_{max}) between these two sarcomere lengths is significantly lower in the *Lmod2* cKO mice, indicating a blunting in myofilament length dependent activation (Fig. 4E). Interestingly, EC_{50}, a measure of the responsiveness of the thin filament to calcium, is not significantly altered at the short sarcomere length, but is significantly decreased when sarcomere length is extended to 2.25 microns in the cKO mice (Fig. 4A, B insets). This indicates an increase in calcium sensitivity at the longer sarcomere length in the cKO mice.

This enhancement of the EC_{50} of calcium activation could be indicative of an alteration in phosphorylation levels of myofilament proteins and/or titin [25–29]. However, total phosphorylation of several myofilament proteins, including TnI, and myosin light chain 2 (MLC2), is not altered following loss of Lmod2 (Fig. 5). Phosphorylation of cardiac troponin T (cTnT) is significantly reduced in the cKO mice, but only when compared to $Lmod2^{fl/fl}$;$MCM^{+/-}$ vehicle-treated mice. Total phosphorylation of MyBP-C is increased, which could indicate a compensatory attempt to alter contractility. Consistent with the total phosphorylation results, phosphorylation of cTnI at a well-described protein kinase A site (Ser23/24) is unchanged in the cKO (Fig S4).

To determine if the force deficit observed in the trabeculae is predominantly due to a defect in cell-to-cell force transmission or myofilament force generation, we generated force/Ca^{2+} curves using single cells isolated from intraventricular septums of mice used in the fiber experiments. Since the results of the fiber mechanics were identical in all three control groups (see above), we focused on the vehicle-treated $Lmod2^{+/+}$;$MCM^{+/-}$ mice as a control in the single cell experiments. The control cells produce significantly more force than the cKO cells (Fig. 6A, B, Table S1). Thus, the deficit in force production occurs at the myofilament level. Unlike the trabeculae, the knockout cells have roughly the same response to calcium as the control cells (i.e., no shift in EC_{50}). This indicates that the shift in calcium sensitivity upon Lmod2 knockout only occurs at the level of the fiber. To better understand the functional overlap of thin and thick filaments in cKO hearts we set out to determine force

production at long sarcomere lengths (i.e., analyze the descending limb of the length-tension curve). Starting at a sarcomere length of 2.25 ± 0.03 μm, control and cKO cells were stretched and maximally activated until active force was no longer generated. We found that, on average, control cells produce no force at a sarcomere length of 3.62 μm, while cKO cells produce no force at 3.38 μm (Fig. 6C). This result corresponds to ~12% decrease in thin filament length. The cKO cells also have a significantly altered descending limb slope ($p<0.0001$), which suggests that force is depressed independent of a decrease in thin filament length.

3.4. Lmod2 levels are directly linked to thin filament length and cardiac function in vivo

We next set out to determine if thin filament length is linked to the amount of Lmod2 present, cardiac function and contractile force generation. In order to vary Lmod2 levels, we injected the *Lmod2*$^{fl/fl}$;MCM$^{+/-}$ mice with 10, 15 or 20 mg/kg of tamoxifen on 3 consecutive days and compared these mice to those with a complete loss of Lmod2 (30 mg/kg) and mice injected with vehicle alone (0 mg/kg). Note, the vehicle injected mice have reduced levels of Lmod2 but no change in thin filament lengths or cardiac function (**Figs. 1, 2, 4**). We found a significant negative correlation between the amount of tamoxifen injected and Lmod2 levels ($p = 0.0059$), thin filament length ($p = 0.0059$), systolic performance (EF) ($p = 0.021$) and maximum calcium activated force production ($p = 0.013$) (Fig. 7A). Furthermore, there is a positive correlation between thin filament length and both systolic performance (EF) ($p < 0.0001$) and maximum calcium activated force production ($p = 0.0013$) (Fig. 7B). These results indicate that a dose response relationship exists between Lmod2 and thin filament length, as well as cardiac function, *in vivo*.

4. Discussion

We previously generated a constitutive *Lmod2* knockout mouse which displays cardiac remodeling as early as postnatal day 6 and dies 2–3 weeks after birth at a point in which the heart is still developing (e.g., in the midst of a shift in expression from fetal to adult isoforms of many myofilament proteins and continued cardiac hypertrophy)[12]. In this study we set out to determine the role Lmod2 plays in the adult heart, and how thin filament length regulation contributes to contractility and cardiac function in the adult mouse. Adult mice are more amenable to studying fiber mechanics and results obtained are not confounded by ongoing developmental processes.

Heart-specific loss of Lmod2 in the adult mouse results in a very rapid loss of systolic performance and death (in less than a week), with nearly no change in cardiac morphology. Thus, we were able to analyze the acute effects of loss of Lmod2 on thin filament length, force production and cardiac function as the cKO heart does not have much time to alter isoforms or remodel.

The rapid disease development in the *Lmod2* cKO mice parallels the constitutive knockout model. In the constitutive knockout mice, cardiac function looks to be normal throughout embryonic development and the first week after birth, then rapidly declines in the following week. We hypothesized that this is a failure of the Lmod2 deficient heart to respond to increased afterload due to increased vascular resistance after the animals are born [12].

Preload also increases as venous return rises upon increases in respiration and skeletal muscle use as the mice become more mobile. Under normal conditions an increase in preload results in an increase in cardiac output (the FrankStarling law of the heart) due to myofilament length-dependent activation (for review see: [30, 31]). However, the Lmod2 cKO mice display a reduction in length-dependent activation (i.e., smaller increase in force output as sarcomere length increases) compared with control mice. Consequently, hearts which lack Lmod2 may be unable to meet the hemodynamic demands of an active mouse. Indeed, upregulation of CARP1 and FHL1 in the cKO point to a heart under biomechanical stress. This could explain the nearly immediate cardiac failure in the adult cKO mice, while the constitutive KO mice die as their activity increases within the first few weeks after birth.

Shorter thin filaments contribute to loss of contractile force in the cKO mice. Based on sliding filament theory, abnormally short thin filaments are predicted to result in a deficit of force production at long sarcomere lengths due to reduced thin-thick filament overlap. A uniform decrease in thin filament length of 10–12% should result in a leftward shift of the SL-tension curve with maximum tension developed at a SL of ~2.0 μm (vs. ~2.3 within the first few weeks after birth. Shorter thin filaments contribute to loss of contractile force in the cKO m in the WT) [32, 33]. Indeed the ckO mice display a leftward shifted descending limb on the SL-tension curve, confirming that thin filaments are shorter. However, the descending limb also has an altered slope, indicating that loss of force is only partly explained by uniformly shorter thin filaments. Although significant, there is only a moderate correlation between thin filament length and maximum calcium activated force production, which also suggests other factor(s) play a role in the loss of contractile force in the cKO. We were also surprised to observe a slight increase in force as SL increases (from 1.95 to 2.25 μm) in the cKO trabeculae. At a SL of 2.25 μm the cKO trabeculae would be predicted to be on the descending limb of the SL-tension curve, which would result in less force than is produced at a SL of 1.95 μm. In these experiments, sarcomere length is set prior to activation with calcium (diastolic). However, it is well documented that diastolic sarcomere length is not maintained during activation of contraction, even though overall muscle length is held isometric. This is the result of internal shortening of sarcomeres due to inherent compliance in the preparation [34–36]. Since we are unable to control for this shortening, the cKO trabeculae activated at a SL of 2.25 μm will reach steady-state tension at an unknown, shorter SL, and, accordingly, a different position on the descending limb of the lengthtension curve. Concurrently, trabeculae activated at a SL of 1.95 μm would move down the ascending limb of the SL-tension curve producing less force than expected. Together, this could explain the apparent lack of a decrease in force at a SL of 2.25 μm in the cKO.

Thin filament non-uniformity could contribute to a decrease in force as an optimal sarcomere length may not exist (i.e., a sarcomere length in which there is no interference due to filaments crossing the H-zone at the same time all of the myosin heads are engaged). Additionally, it is hypothesized that the interaction of MyBP-C with actin aids in the activation of the thin filament [37, 38]. The distribution of MyBP-C is weighted more heavily towards the M-line on the thick filament. Thus, thin filaments that are shorter than “normal” could interact less with MyBP-C along the C-zone, resulting in a depression of force production.

It is unclear what causes the non-uniformity of thin filament lengths. One possibility is that the action of myosin interacting with actin causes small breaks in the thin filament that over time act to reduce the length of the filament, in a nonhomogenous matter, leading to a reduction in force output. Lmod2 could help repair the thin filaments, maintaining their mature, uniform lengths. Alternatively, non-uniformity could arise secondarily to the loss of thin filament length regulation and decrease in contractile force output. Shorter, non-uniform thin filament lengths have been reported following the loss of the giant actin-binding protein nebulin in the skeletal muscle of mice and in humans [39, 40]. The non-uniformity in the nebulin knockout mice has been proposed to result from muscle use over time since thin filaments were uniformly shorter when measured right after birth [41, 42].

Lmod2 functions biochemically as a potent nucleator *in vitro* and is required to maintain mature thin filament lengths in cells and *in vivo* [10, 12]. Consistent with these functions, the cKO mice have a significant decrease in the levels of thin filament proteins, whereas thick filament and Z-disc components are unchanged. This could be due not only to shorter but also fewer thin filaments, since Lmod2 has been hypothesized to be involved in the turnover of thin filaments [43]. In an attempt to distinguish between these possibilities, we tested whether there are fewer thin filaments in the cKO by measuring the levels of Tmod1. We reasoned that since Tmod1 only interacts with the pointed end of the thin filament [4, 24], the amount of cytoskeletonassociated (i.e., assembled) Tmod1 should be an accurate measure of the number of thin filaments present in sarcomeres. This assumes that Lmod2 does not regulate a population of thin filaments distinct from those capped by Tmod1. We found no significant change in the levels of assembled Tmod1 in the left ventricle of the Lmod2 cKO mice, suggesting little change in thin filament number. We therefore conclude that, Lmod2 functions to maintain the length of existing thin filaments, not in thin filament turnover (at least over the span of a week).

It is intriguing that a nearly 85% reduction in Lmod2 protein leads to no observable phenotype, but a further reduction in Lmod2 levels displays a remarkable dose response relationship with respect to both thin filament length and cardiac function. Corroborating this observation, the *Lmod2* constitutive heterozygous mice (which express ~50% of wild type Lmod2 levels) do not present with cardiac abnormalities ([12], data not shown). We also previously found that expression of GFPLmod2 at ~40% of endogenous *Lmod2* levels in the heart via adeno-associated virus is able to rescue the constitutive *Lmod2* knockout mice [12]. Although the stoichiometry of Lmod2 and the thin filament is unknown, these results suggest a surprisingly minute amount of Lmod2 has a large effect on thin filament assembly and cardiac function.

Lmod2 may affect contractility independent of thin filament length regulation. Previous studies have shown that Lmod2 can directly bind to the side of the actin filament in cells [13, 44] and inhibit myosin ATPase activity *in vitro* [45]. The latter result predicts that loss of Lmod2 would relieve the myosin ATPase inhibition, thereby increasing force output, which is opposite of the decrease in force we observed in the single trabeculae and isolated cardiomyocytes of the cKO mice. Since the *Lmod2* cKO mice display shorter, non-uniform thin filaments, which likely reduces force, it is difficult to determine whether the removal of Lmod2 has any positive affect on force output. The $Lmod2^{fl/fl}$;$MCM^{+/-}$ mice injected with

vehicle alone, which express only ~15% of endogenous Lmod2 levels but have no detectable changes in thin filament structure, provide a model to test the effect of reduction of Lmod2 on contractility. Single trabeculae isolated from these mice do not have a significant change in mean maximum calcium-activated force. Although we could not detect an increase in force upon a reduction in Lmod2, further study is warranted to determine if Lmod2 influences myosin ATPase *in vivo*.

It is unclear what causes an increase in sensitivity to calcium in the *Lmod2* cKO trabeculae at a sarcomere length of 2.25 μm. If an alteration in phosphorylation of thin filament regulatory components brought about the change in sensitivity, then we would expect to see a similar change in single cell experiments, which shows no difference in calcium sensitivity. One possibility is that the shift in EC_{50} of calcium activation observed in the trabeculae is due to a heterogeneous mixture of cells within the cardiac tissue. We observed a greater variation in single-cell forces in the cKO compared to the control, with some cells producing nearly normal levels of force while others producing very little force. Since cardiomyocytes function in series within the fiber, low force producing cells could effectively cap the maximal force production of the fiber, while higher force producing cells could contribute relatively more force at submaximal calcium levels. We hypothesize that the combination of high and low force producing cells produces a shift in the EC_{50} of calcium activation that is only observed in the trabeculae. The increased variation of single-cell forces in the cKO could result from variation in the efficiency of tamoxifen to induce recombination [e.g.,46].

In conclusion, loss of Lmod2 in adult mice results in a rapid loss of contractile force and cardiac failure. Our results indicate that Lmod2 functions to maintain thin filament length and uniformity, which contributes to proper contractile force generation.

Supplementary Material

Refer to Web version on PubMed Central for supplementary material.

Acknowledgments

We thank David O'Neil Lyons, Greg Lyons, and Max Zelikovsky for assistance with mouse colony maintenance and genotyping, Marissa Lopez-Pier for technical assistance, Drs. Miensheng Chu and Stefanie Novak for insightful discussions, Dr. Joshua Strom in the Small Animal Phenotyping Core at the University of Arizona for assistance with echocardiography and Drs. Tom Doetschman and Teodora Georgieva in the GEMM Core at the University of Arizona for generating the *Lmod2* conditional knockout mouse. This work was supported by NIH R01HL123078 and a donation from Linda and Jim Lee (C.C.G.), as well as the American Heart Association 16GRNT31390006 (J.P.K.). Support was also received from the Sarver Heart Center at the University of Arizona and the Steven M. Gootter Foundation.

References Cited

[1]. Winter JM, Joureau B, Lee EJ, Kiss B, Yuen M, Gupta VA, Pappas CT, Gregorio CC, Stienen GJ, Edvardson S, Wallgren-Pettersson C, Lehtokari VL, Pelin K, Malfatti E, Romero NB, Engelen BG, Voermans NC, Donkervoort S, Bonnemann CG, Clarke NF, Beggs AH, Granzier H, Ottenheijm CA, Mutation-specific effects on thin filament length in thin filament myopathy, Ann Neurol 79(6) (2016) 959–69. [PubMed: 27074222]

[2]. Yuen M, Sandaradura SA, Dowling JJ, Kostyukova AS, Moroz N, Quinlan KG, Lehtokari VL, Ravenscroft G, Todd EJ, Ceyhan-Birsoy O, Gokhin DS, Maluenda J, Lek M, Nolent F, Pappas

CT, Novak SM, D'Amico A, Malfatti E, Thomas BP, Gabriel SB, Gupta N, Daly MJ, Ilkovski B, Houweling PJ, Davidson AE, Swanson LC, Brownstein CA, Gupta VA, Medne L, Shannon P, Martin N, Bick DP, Flisberg A, Holmberg E, Van den Bergh P, Lapunzina P, Waddell LB, Sloboda DD, Bertini E, Chitayat D, Telfer WR, Laquerriere A, Gregorio CC, Ottenheijm CA, Bonnemann CG, Pelin K, Beggs AH, Hayashi YK, Romero NB, Laing NG, Nishino I, Wallgren-Pettersson C, Melki J, Fowler VM, MacArthur DG, North KN, Clarke NF, Leiomodin-3 dysfunction results in thin filament disorganization and nemaline myopathy, J Clin Invest 124(11) (2014) 4693–708. [PubMed: 25250574]

[3]. Conley CA, Fritz-Six KL, Almenar-Queralt A, Fowler VM, Leiomodins: larger members of the tropomodulin (Tmod) gene family, Genomics 73(2) (2001) 127–39. [PubMed: 11318603]

[4]. Weber A, Pennise CR, Babcock GG, Fowler VM, Tropomodulin caps the pointed ends of actin filaments, J Cell Biol 127(6 Pt 1) (1994) 1627–35. [PubMed: 7798317]

[5]. Kostyukova AS, Choy A, Rapp BA, Tropomodulin binds two tropomyosins: a novel model for actin filament capping, Biochemistry 45(39) (2006) 12068–75. [PubMed: 17002306]

[6]. Gregorio CC, Fowler VM, Mechanisms of thin filament assembly in embryonic chick cardiac myocytes: tropomodulin requires tropomyosin for assembly, J Cell Biol 129(3) (1995) 683–95. [PubMed: 7730404]

[7]. Rao JN, Madasu Y, Dominguez R, Mechanism of actin filament pointed-end capping by tropomodulin, Science 345(6195) (2014) 463–7. [PubMed: 25061212]

[8]. Boczkowska M, Rebowski G, Kremneva E, Lappalainen P, Dominguez R, How Leiomodin and Tropomodulin use a common fold for different actin assembly functions, Nat Commun 6 (2015) 8314. [PubMed: 26370058]

[9]. Ly T, Moroz N, Pappas CT, Novak SM, Tolkatchev D, Wooldridge D, Mayfield RM, Helms G, Gregorio CC, Kostyukova AS, The N-terminal tropomyosin- and actin-binding sites are important for leiomodin 2's function, Mol Biol Cell 27(16) (2016) 2565–75. [PubMed: 27307584]

[10]. Chereau D, Boczkowska M, Skwarek-Maruszewska A, Fujiwara I, Hayes DB, Rebowski G, Lappalainen P, Pollard TD, Dominguez R, Leiomodin is an actin filament nucleator in muscle cells, Science 320(5873) (2008) 239–43. [PubMed: 18403713]

[11]. Yamashiro S, Speicher KD, Speicher DW, Fowler VM, Mammalian tropomodulins nucleate actin polymerization via their actin monomer binding and filament pointed endcapping activities, J Biol Chem 285(43) (2010) 33265–80. [PubMed: 20650902]

[12]. Pappas CT, Mayfield RM, Henderson C, Jamilpour N, Cover C, Hernandez Z, Hutchinson KR, Chu M, Nam KH, Valdez JM, Wong PK, Granzier HL, Gregorio CC, Knockout of Lmod2 results in shorter thin filaments followed by dilated cardiomyopathy and juvenile lethality, Proc Natl Acad Sci U S A 112(44) (2015) 13573–8. [PubMed: 26487682]

[13]. Tsukada T, Pappas CT, Moroz N, Antin PB, Kostyukova AS, Gregorio CC, Leiomodin-2 is an antagonist of tropomodulin-1 at the pointed end of the thin filaments in cardiac muscle, J Cell Sci 123(Pt 18) (2010) 3136–45. [PubMed: 20736303]

[14]. Sohal DS, Nghiem M, Crackower MA, Witt SA, Kimball TR, Tymitz KM, Penninger JM, Molkentin JD, Temporally regulated and tissue-specific gene manipulations in the adult and embryonic heart using a tamoxifen-inducible Cre protein, Circ Res 89(1) (2001) 20–5. [PubMed: 11440973]

[15]. Farman GP, Walker JS, de Tombe PP, Irving TC, Impact of osmotic compression on sarcomere structure and myofilament calcium sensitivity of isolated rat myocardium, Am J Physiol Heart Circ Physiol 291(4) (2006) H1847–55. [PubMed: 16751283]

[16]. Fan D, Wannenburg T, de Tombe PP, Decreased myocyte tension development and calcium responsiveness in rat right ventricular pressure overload, Circulation 95(9) (1997) 23127.

[17]. Kentish JC, ter Keurs HE, Ricciardi L, Bucx JJ, Noble MI, Comparison between the sarcomere length-force relations of intact and skinned trabeculae from rat right ventricle. Influence of calcium concentrations on these relations, Circ Res 58(6) (1986) 755–68. [PubMed: 3719928]

[18]. Littlefield R, Fowler VM, Measurement of thin filament lengths by distributed deconvolution analysis of fluorescence images, Biophys J 82(5) (2002) 2548–64. [PubMed: 11964243]

[19]. Gokhin DS, Fowler VM, Software-based measurement of thin filament lengths: an opensource GUI for Distributed Deconvolution analysis of fluorescence images, J Microsc 265(1) (2017) 11–20. [PubMed: 27644080]

[20]. Lexow J, Poggioli T, Sarathchandra P, Santini MP, Rosenthal N, Cardiac fibrosis in mice expressing an inducible myocardial-specific Cre driver, Dis Model Mech 6(6) (2013) 1470–6. [PubMed: 23929940]

[21]. Sheikh F, Raskin A, Chu PH, Lange S, Domenighetti AA, Zheng M, Liang X, Zhang T, Yajima T, Gu Y, Dalton ND, Mahata SK, Dorn GW, 2nd, Brown JH, Peterson KL, Omens JH, McCulloch AD, Chen J, An FHL1-containing complex within the cardiomyocyte sarcomere mediates hypertrophic biomechanical stress responses in mice, J Clin Invest 118(12) (2008) 3870–80. [PubMed: 19033658]

[22]. Mikhailov AT, Torrado M, The enigmatic role of the ankyrin repeat domain 1 gene in heart development and disease, Int J Dev Biol 52(7) (2008) 811–21. [PubMed: 18956313]

[23]. Kolb J, Li F, Methawasin M, Adler M, Escobar YN, Nedrud J, Pappas CT, Harris SP, Granzier H, Thin filament length in the cardiac sarcomere varies with sarcomere length but is independent of titin and nebulin, J Mol Cell Cardiol 97 (2016) 286–94. [PubMed: 27139341]

[24]. Fowler VM, Sussmann MA, Miller PG, Flucher BE, Daniels MP, Tropomodulin is associated with the free (pointed) ends of the thin filaments in rat skeletal muscle, J Cell Biol 120(2) (1993) 411–20. [PubMed: 8421055]

[25]. Fukuda N, Wu Y, Nair P, Granzier HL, Phosphorylation of titin modulates passive stiffness of cardiac muscle in a titin isoform-dependent manner, J Gen Physiol 125(3) (2005) 257–71. [PubMed: 15738048]

[26]. Konhilas JP, Irving TC, Wolska BM, Jweied EE, Martin AF, Solaro RJ, de Tombe PP, Troponin I in the murine myocardium: influence on length-dependent activation and interfilament spacing, J Physiol 547(Pt 3) (2003) 951–61. [PubMed: 12562915]

[27]. Michael JJ, Gollapudi SK, Chandra M, Effects of pseudo-phosphorylated rat cardiac troponin T are differently modulated by alpha- and beta-myosin heavy chain isoforms, Basic Res Cardiol 109(6) (2014) 442.

[28]. Yamasaki R, Wu Y, McNabb M, Greaser M, Labeit S, Granzier H, Protein kinase A phosphorylates titin's cardiac-specific N2B domain and reduces passive tension in rat cardiac myocytes, Circ Res 90(11) (2002) 1181–8. [PubMed: 12065321]

[29]. Belin RJ, Sumandea MP, Allen EJ, Schoenfelt K, Wang H, Solaro RJ, de Tombe PP, Augmented protein kinase C-alpha-induced myofilament protein phosphorylation contributes to myofilament dysfunction in experimental congestive heart failure, Circ Res 101(2) (2007) 195–204. [PubMed: 17556659]

[30]. de Tombe PP, Mateja RD, Tachampa K, Ait Mou Y, Farman GP, Irving TC, Myofilament length dependent activation, J Mol Cell Cardiol 48(5) (2010) 851–8. [PubMed: 20053351]

[31]. Kobirumaki-Shimozawa F, Inoue T, Shintani SA, Oyama K, Terui T, Minamisawa S, Ishiwata S, Fukuda N, Cardiac thin filament regulation and the Frank-Starling mechanism, J Physiol Sci 64(4) (2014) 221–32. [PubMed: 24788476]

[32]. Granzier HL, Akster HA, Ter Keurs HE, Effect of thin filament length on the forcesarcomere length relation of skeletal muscle, Am J Physiol 260(5 Pt 1) (1991)C1060–70. [PubMed: 2035614]

[33]. Allen DG, Kentish JC, The cellular basis of the length-tension relation in cardiac muscle, J Mol Cell Cardiol 17(9) (1985) 821–40. [PubMed: 3900426]

[34]. Huxley HE, Stewart A, Sosa H, Irving T, X-ray diffraction measurements of the extensibility of actin and myosin filaments in contracting muscle, Biophys J 67(6) (1994)241121.

[35]. Konhilas JP, Irving TC, de Tombe PP, Length-dependent activation in three striated muscle types of the rat, J Physiol 544(Pt 1) (2002) 225–36. [PubMed: 12356894]

[36]. Wakabayashi K, Sugimoto Y, Tanaka H, Ueno Y, Takezawa Y, Amemiya Y, X-ray diffraction evidence for the extensibility of actin and myosin filaments during muscle contraction, Biophys J 67(6) (1994) 2422–35. [PubMed: 7779179]

[37]. Mun JY, Previs MJ, Yu HY, Gulick J, Tobacman LS, Beck Previs S, Robbins J, Warshaw DM, Craig R, Myosin-binding protein C displaces tropomyosin to activate cardiac thin filaments and

governs their speed by an independent mechanism, Proc Natl Acad Sci U S A 111(6) (2014) 2170–5. [PubMed: 24477690]

[38]. Razumova MV, Shaffer JF, Tu AY, Flint GV, Regnier M, Harris SP, Effects of the Nterminal domains of myosin binding protein-C in an in vitro motility assay: Evidence for longlived cross-bridges, J Biol Chem 281(47) (2006) 35846–54. [PubMed: 17012744]

[39]. Witt CC, Burkart C, Labeit D, McNabb M, Wu Y, Granzier H, Labeit S, Nebulin regulates thin filament length, contractility, and Z-disk structure in vivo, EMBO J 25(16) (2006) 3843–55. [PubMed: 16902413]

[40]. Ottenheijm CA, Witt CC, Stienen GJ, Labeit S, Beggs AH, Granzier H, Thin filament length dysregulation contributes to muscle weakness in nemaline myopathy patients with nebulin deficiency, Hum Mol Genet 18(13) (2009) 2359–69. [PubMed: 19346529]

[41]. Littlefield RS, Fowler VM, Thin filament length regulation in striated muscle sarcomeres: pointed-end dynamics go beyond a nebulin ruler, Semin Cell Dev Biol 19(6) (2008) 511–9. [PubMed: 18793739]

[42]. Bang ML, Li X, Littlefield R, Bremner S, Thor A, Knowlton KU, Lieber RL, Chen J, Nebulin-deficient mice exhibit shorter thin filament lengths and reduced contractile function in skeletal muscle, J Cell Biol 173(6) (2006) 905–16. [PubMed: 16769824]

[43]. Fowler VM, Dominguez R, Tropomodulins and Leiomodins: Actin Pointed End Caps and Nucleators in Muscles, Biophys J 112(9) (2017) 1742–1760. [PubMed: 28494946]

[44]. Skwarek-Maruszewska A, Boczkowska M, Zajac AL, Kremneva E, Svitkina T, Dominguez R, Lappalainen P, Different localizations and cellular behaviors of leiomodin and tropomodulin in mature cardiomyocyte sarcomeres, Mol Biol Cell 21(19) (2010) 3352–61. [PubMed: 20685966]

[45]. Szatmari D, Bugyi B, Ujfalusi Z, Grama L, Dudas R, Nyitrai M, Cardiac leiomodin2 binds to the sides of actin filaments and regulates the ATPase activity of myosin, PLoS One 12(10) (2017) e0186288. [PubMed: 29023566]

[46]. Bersell K, Choudhury S, Mollova M, Polizzotti BD, Ganapathy B, Walsh S, Wadugu B, Arab S, Kuhn B, Moderate and high amounts of tamoxifen in alphaMHC-MerCreMer mice induce a DNA damage response, leading to heart failure and death, Dis Model Mech 6(6) (2013) 1459–69. [PubMed: 23929941]

Highlights

- Loss of actin-binding protein Lmod2 in adult mice results in rapid cardiac failure.
- Cardiomyocytes without Lmod2 have a severe reduction in contractile force.
- Shorter, non-uniform actin-thin filaments contribute to loss of contractile force.

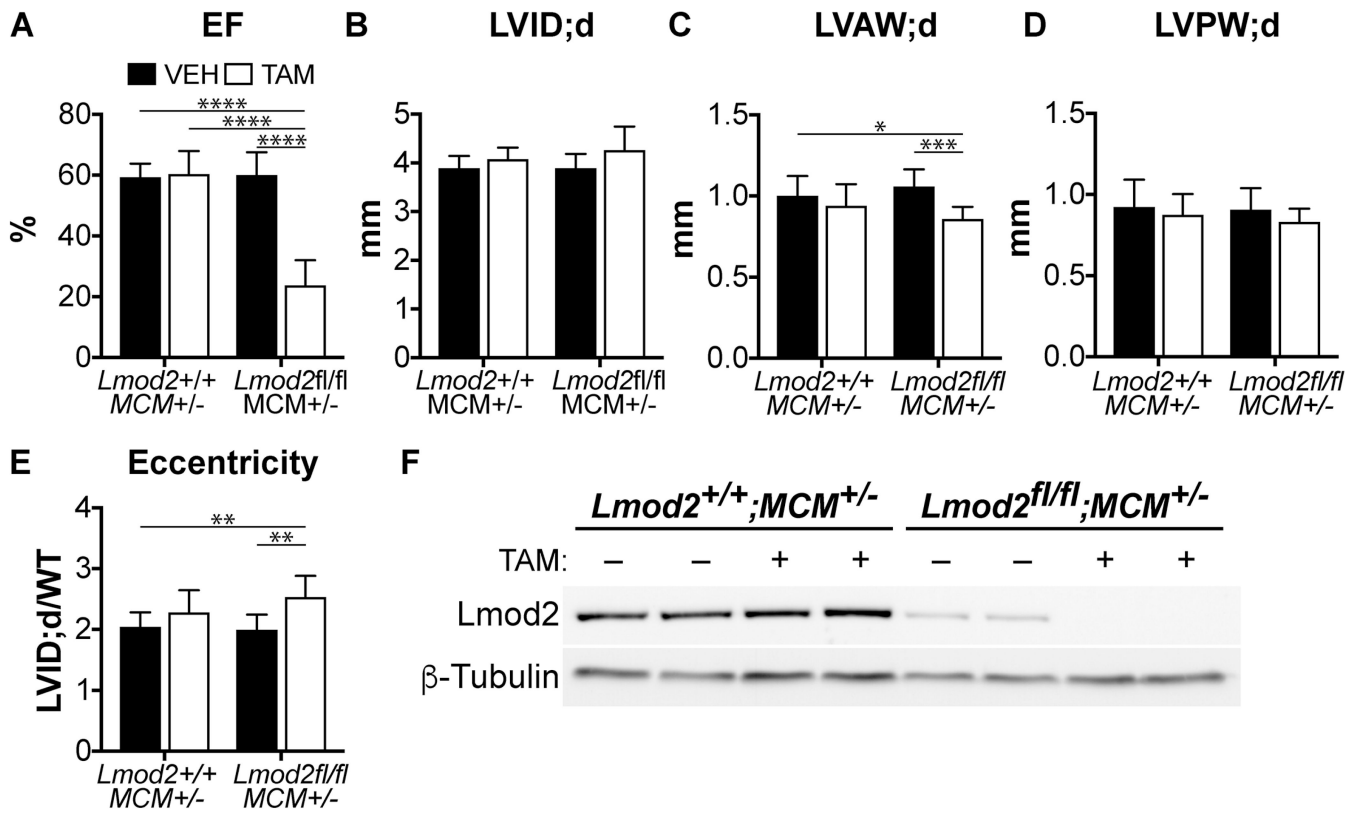

Figure 1. Knockout of Lmod2 results in impaired left ventricle systolic performance.

(A-E) Echocardiography analysis of vehicle (black bars) or tamoxifen (white bars) treated mice. (A) Ejection fraction; **(B)** Left ventricle internal dimension in diastole; **(C)** Left ventricle anterior wall thickness in diastole; **(D)** Left ventricle posterior wall thickness in diastole; and **(E)** Eccentricity index, which equals the left ventricle internal dimension in diastole divided by the sum of the anterior and posterior wall thicknesses. All values represent means ± SD; n = 8–12. **(F)** Immunoblot of LV lysate from mice 7 days after the first injection of vehicle (−) or tamoxifen (+). Lysate was probed with antibodies to Lmod2 and β-tubulin.

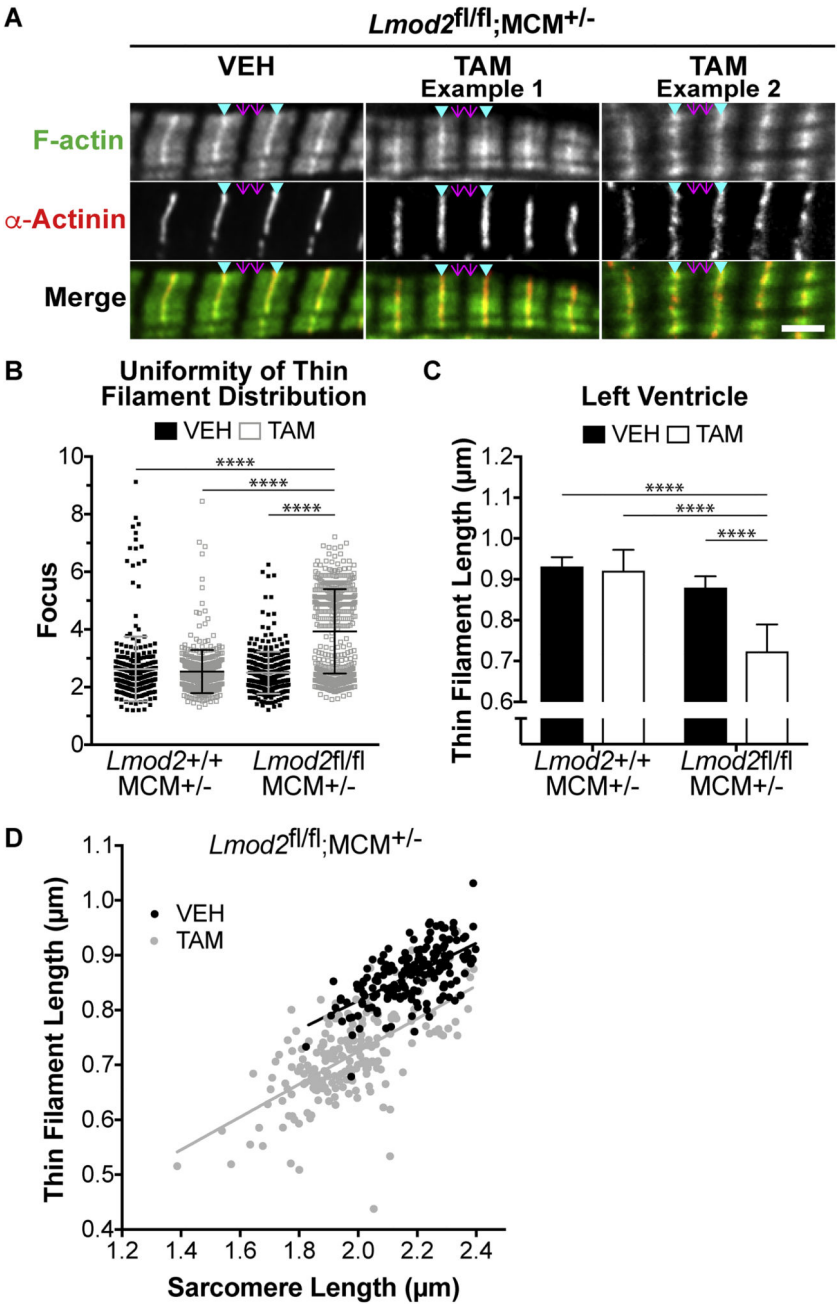

Figure 2. Cardiac thin filament length is reduced in the *Lmod2* cKO mice.

(A) Representative images of immunofluorescence staining of LV free wall in vehicle and tamoxifen treated *Lmod2*$^{fl/fl}$;MCM$^{+/-}$ mice. F-actin is in green and α-actinin, which marks the Z-disc, is in red in the merged images. The locations of thin filament barbed (arrowheads) and pointed (arrows) ends are indicated. Scale bar = 2 μm. Examples of uniform (1) and non-uniform (2) thin filaments upon tamoxifen treatment are shown. **(B)** Mean focus values, which represents the uniformity of thin filament lengths within each sarcomere (the smaller the number the more uniform the filament lengths). **(C)** Thin filament length in LV free wall of vehicle (black bars) and tamoxifen (white bars) treated

mice. All values are means ± SD; n = 8–12. **(D)** Thin filament length plotted against sarcomere length for *Lmod2*$^{fl/fl}$;MCM$^{+/-}$ mice treated with vehicle (black circles) or tamoxifen (grey circles). The slopes of the two linear regression lines are significantly non-zero ($p < 0.0001$) and not significantly different from each other. The y-intercept of the TAM-treated linear regression line is significantly lower ($p < 0.0001$) than the control, indicating thin filaments are shorter when sarcomere length is taken into account.

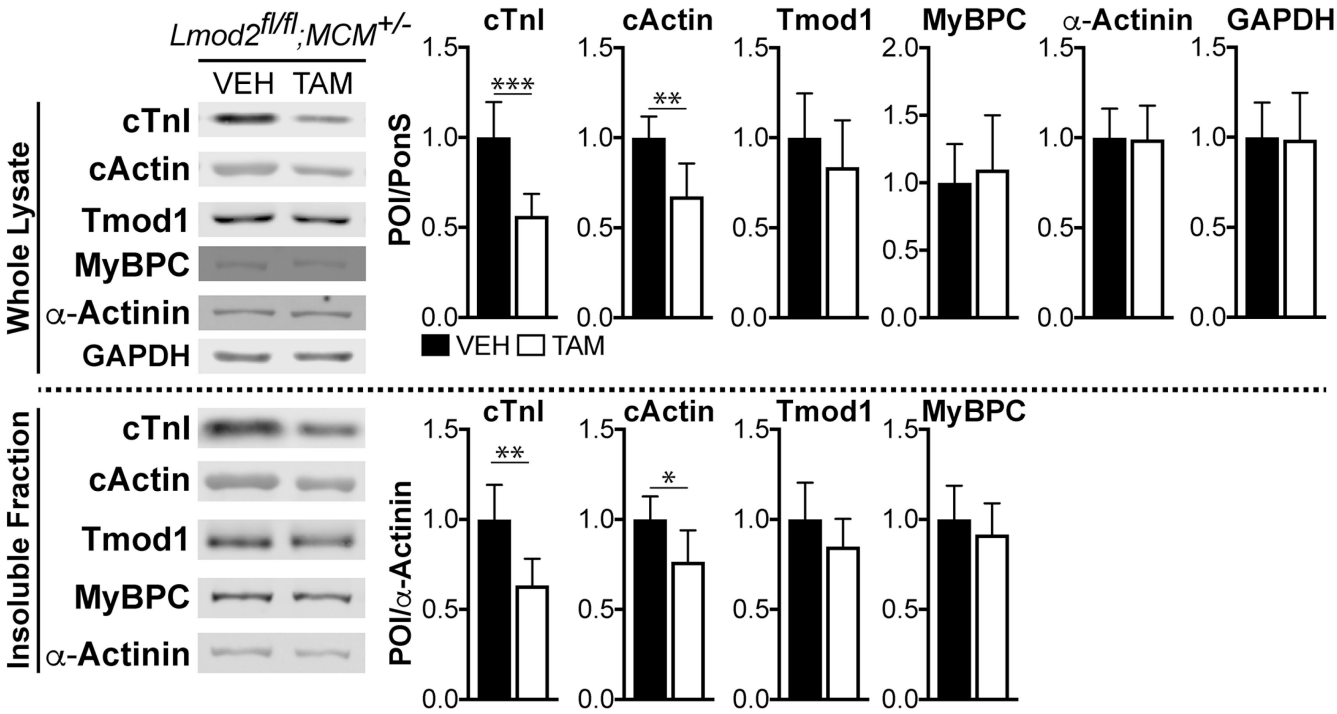

Figure 3. The levels of thin filament components are significantly reduced in the LV of *Lmod2* cKO mice.

Immunoblot analysis of LV proteins in whole cell lysate (top panel) or insoluble fraction (bottom panel) of *Lmod2*$^{fl/fl}$;MCM$^{+/-}$ mice treated with vehicle (black bars) or tamoxifen (white bars). (Left) Single representative blots; (Right) Mean relative protein levels following normalization to total protein via Ponceau S staining. Error bars indicate the SD, n = 5–8.

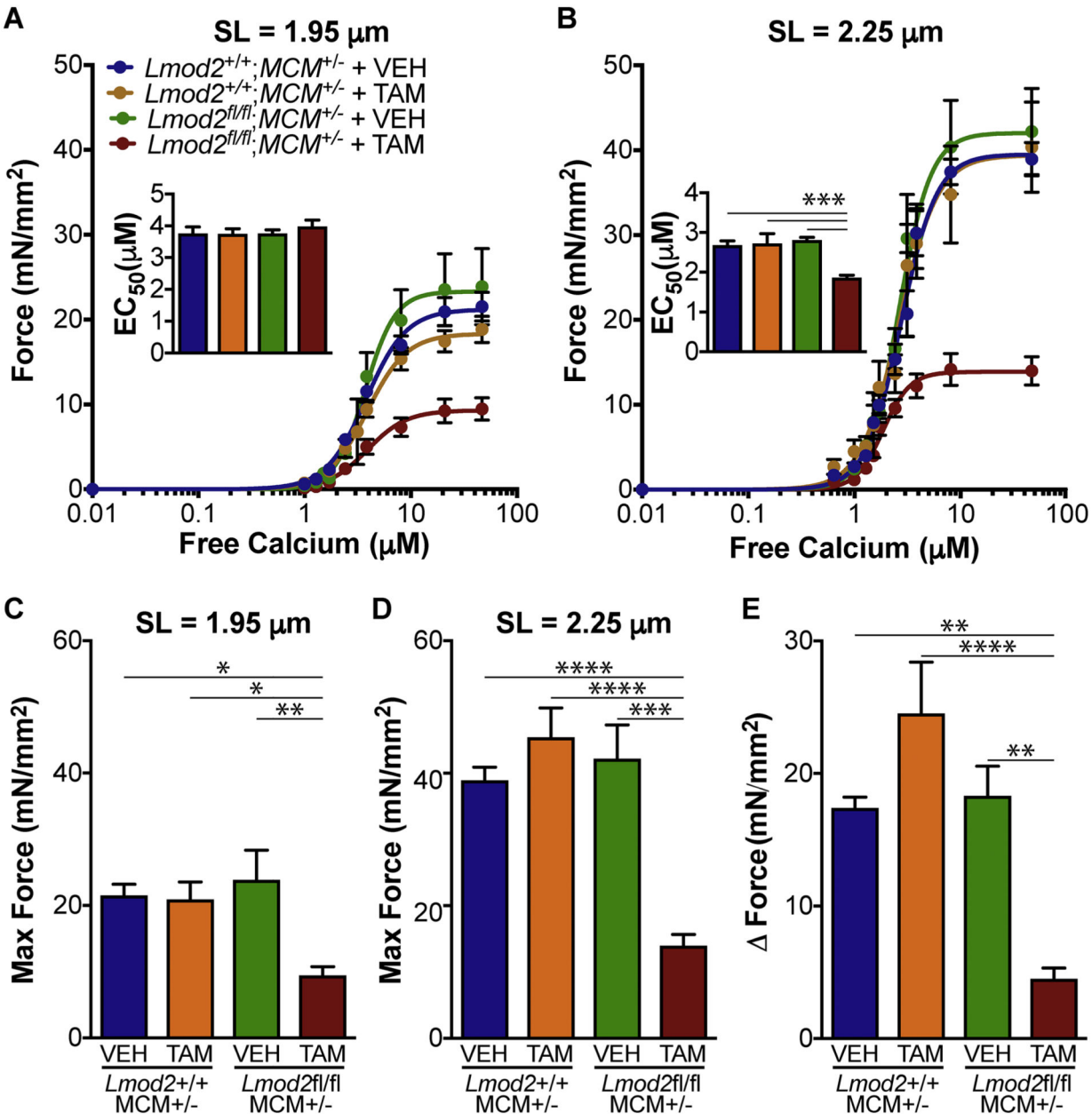

Figure 4. Loss of Lmod2 reduces calcium-activated force and alters calcium sensitivity in cardiac trabeculae.

Force-Ca^{2+} relationship of cardiac trabeculae at short (1.95 μm-**A**) and long (2.25 μm-**B**) sarcomere lengths. The insets are graphs of the mean EC_{50} of calcium activation. Maximum calcium-activated force at sarcomere lengths 1.95 μm **(C)** and 2.25 μm **(D)**. **(E)** Change in maximum force as sarcomere length increases. All values are means ± SEM; n = 5–6.

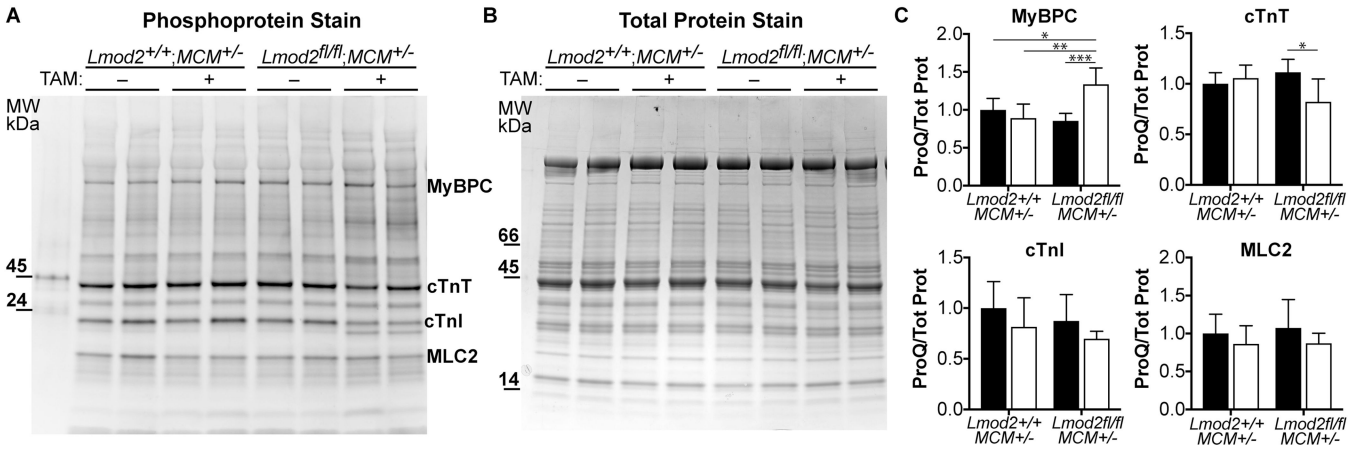

Figure 5. Total phosphorylation of thin filament regulatory proteins is not significantly changed.

(A) Representative gel of LV lysate stained for total phosphoprotein content. **(B)** Corresponding Coomassie blue stain for total protein. **(C)** Mean phosphoprotein levels normalized to total protein for mice treated with vehicle (black bars) or tamoxifen (white bars). Error bars indicate the SD, n = 5–6.

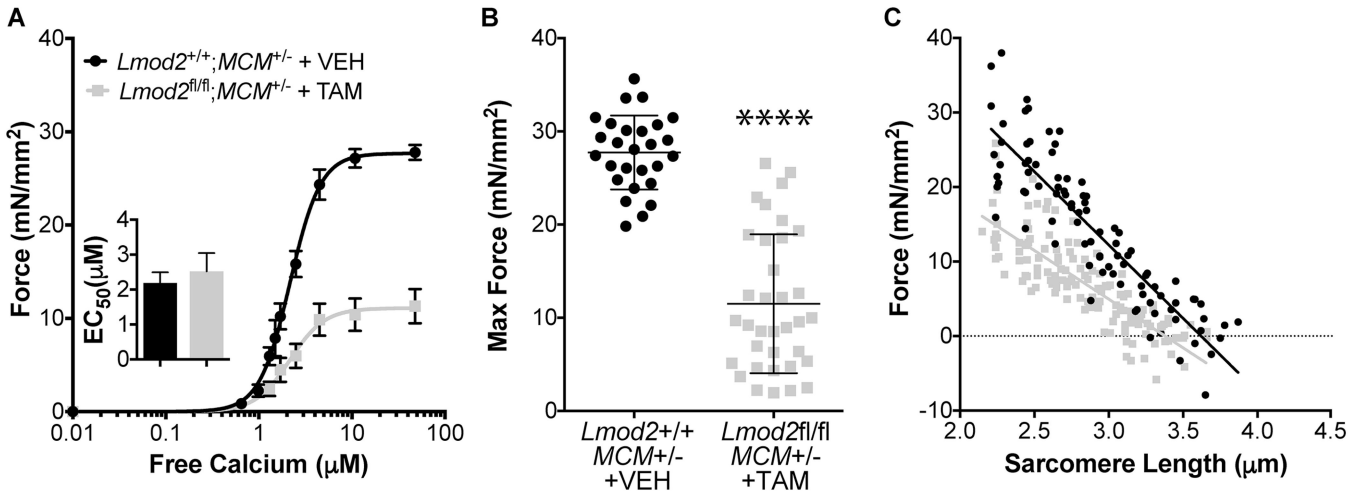

Figure 6. Calcium activated contractile force is reduced in cardiomyocytes isolated from *Lmod2* cKO mice.

(A) Force-Ca^{2+} relationship of cardiac cells at a sarcomere length of 2.25 μm. The inset is a graph of mean EC_{50} of calcium activation. **(B)** Mean force at maximum calcium activation at 2.25 μm. Error bars indicate ± SEM; n = 27–35 cells from 5–6 animals. **(C)** Maximum calcium-activated force at various sarcomere lengths. n = 15 cells from 5 WT animals and 27 cells from 6 cKO animals.

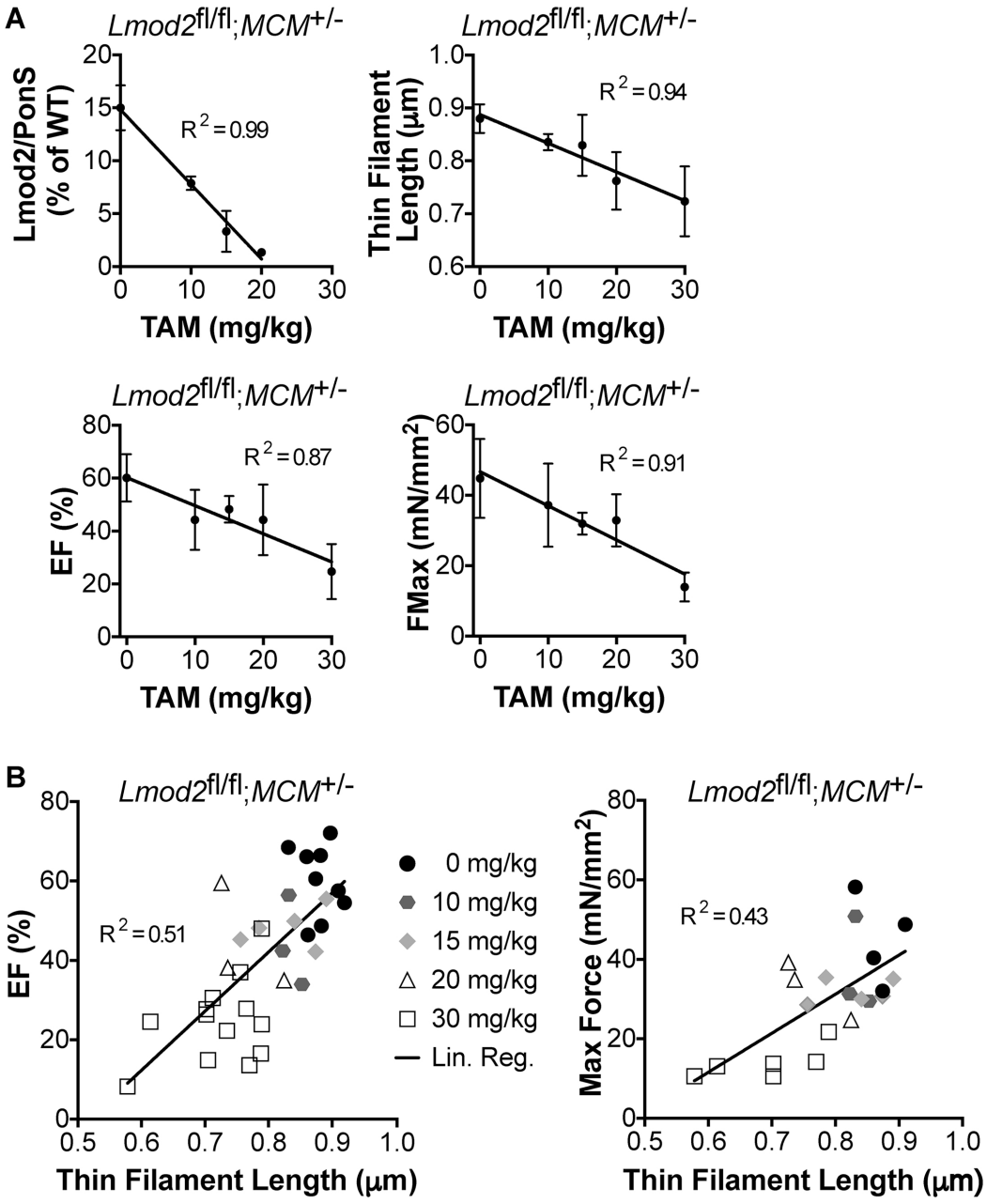

Figure 7. Thin filament length and cardiac function negatively correlate with tamoxifen dose; cardiac function positively correlates with thin filament length.

(A) Relative Lmod2 levels, thin filament (TF) length, ejection fraction (EF) and maximal activated force (FMax) plotted against the dose of tamoxifen (TAM) injected. 0 mg/kg are mice injected with vehicle alone. Data were fit using linear regression. All values are means ± SD; n = 3–13 animals. **(B)** Ejection fraction (EF) and maximal calcium activated force (FMax) plotted against thin filament length. n = 3–13 animals.